

# Probabilistic Force Estimation and Contact Detection for Quadrupedal Robot Locomotion

Mehdi Zarei, Mohammadreza Gilak, Saman Samiei, Mohammad Hossein Basiri\*, Mohammad Mehdi Jalalmaab, Behzad Ahi, Hassan Haddadpour

**Abstract**—Accurate contact state estimation is fundamental to achieving stable locomotion in legged robots. Force sensors are notoriously unreliable and prone to performance degradation over time, and traditional heuristic approaches frequently fail on slippery or unstructured terrain. Disturbance observer-based methods have demonstrated promising performance in contact state estimation; however, they often depend on extensive empirical tuning. The interacting multiple model Kalman filter has emerged as a powerful framework for representing robot motion as a switched system of contact modes, yet existing implementations typically assume a constant transition probability matrix. This paper introduces a novel probabilistic contact estimation framework for a quadrupedal leg based on an interacting multiple model Kalman filter with a newly designed time-varying transition probability matrix. In contrast to static formulations, the proposed matrix adapts dynamically according to real-time kinematic information and gait phase progression, thereby enabling more responsive transitions among swing, stance, and collision modes. In addition, a terrain uncertainty parameter has been included, which can be tuned to enhance performance in unstructured terrains. Simulation and hardware experiments validate the proposed approach and demonstrate that the method reduces detection latency while improving the robustness of contact state identification relative to traditional baselines. The proposed method has been fully implemented and is available online<sup>1</sup>.

## I. INTRODUCTION

Accurate contact state estimation is a prerequisite to the agile and stable locomotion of quadrupedal robots. The detection of swing, stance, and collision has direct implications for state estimation, control and foothold adaptation [1]. Errors in contact detection cascade through the control hierarchy, causing imbalance, foot slippage, or loss of stability [2]. Contact estimation, therefore, forms the basis of locomotion [3].

Although direct sensing using force or tactile sensors presents a trivial solution, such hardware is impractical

Mehdi Zarei is with the Department of Mechanical Engineering, Sharif University of Technology, Mohammadreza Gilak and Behzad Ahi are with the Department of Electrical Engineering, Sharif University of Technology, Saman Samiei and Hassan Haddadpour are with the Department of Aerospace Engineering, Sharif University of Technology, Mohammad Hossein Basiri is with the Department of Electrical Engineering, Amirkabir University of Technology, and Mohammad Mehdi Jalalmaab is with the Fasta Robotics Inc. Email: {mehdi.zar@student., mohammadreza.gilak@ee., saman.samiei@ae., ahi@, haddadpour@}sharif.edu, basiri@aut.ac.ir, mjalalmaab@fasta.technology.

\* Corresponding author

<sup>1</sup>Code repository: <https://github.com/FastaRobotics/Probabilistic-Force-Estimation-and-Contact-Detection-for-Quadrupedal-Robot-Locomotion>.

in legged platforms. Force sensors are unreliable and suffer from drifting, mechanical deterioration, temperature interference, and structural flexibility [4]–[6], all of which compound into decreasing measurement fidelity over time. Finally, dedicated force sensors at the foot are costlier, require more wiring, and present more critical failure points [7]. These limitations necessitate the development of proprioceptive and model-based estimation techniques to detect the external force and contact states without dedicated hardware [8].

Within this context, the Generalized Momentum-based disturbance Observer (GMO) offers a theoretically grounded approach to estimating the external force based solely on joint position, velocity and torque data [9]. Thresholds on these estimated forces can then be used to detect contact [10]–[12]. For example, in [13], the authors use a discriminative logit model to calculate the probability of contact given an estimated force. However, the generated force estimate using this method is very susceptible to noise and inaccuracies in the robot’s model. To address these challenges, first-order continuous-time [9] and discrete-time [14] filters have been proposed. Probabilistic approaches have also been investigated; for instance, [15] employs a Kalman filter that augments the state with a simple dynamic model of the external force. Additionally, approximate inverse-dynamics forces have been utilized to estimate whether a foothold is sufficiently stable for reliable state estimation [13]. However, all of these methods result in a non-zero force estimate during the swing phase, which can cause unwanted mode switching [16]. In addition, a single linear model cannot capture the swing, stance, and collision modes simultaneously when the contact transitions are abrupt.

The Interacting Multiple-Model Kalman Filter (IMM-KF) provides a structured formulation to overcome the aforementioned limitation by using switched linear system with discrete mode to represent locomotion [17]. Modes correspond to an explicit contact hypothesis, and there are a number of Kalman filters running in parallel, weighted by the mode probabilities provided by a Markov chain. The modes are mixed probabilistically and updated using a likelihood argument to enable simultaneous force estimation and mode detection under the IMM framework [18]. Equally, the implemented solutions have typically assumed a constant transition probability matrix (TPM).

The strength of the IMM framework is its modularity and probabilistic interpretability. The transition probability

matrix can, in principle, consider other sources of information apart from the proprioceptive signals. For example, exteroceptive sensors, gait schedulers or terrain classifiers may be incorporated into the transition probability matrix in a context-aware manner. The additional information could be embedded into a time-varying transition probability matrix so that the estimator can anticipate valid intermittent mode switches and inhibit unlikely mode switches altogether. Thus, the flexibility of IMM formulation is suited for legged systems under uncertainty and changing environments.

Based on this, the present work takes on a simplified yet effective approach to further improve transition modeling. Instead of manually tuning constant probabilities, a more effective approach to transition modeling is employed here, based on the progression of gait phases and easily accessible kinematic clues. Basically, kinematic information and the estimation of force are both included in constructing the transition probability matrix. This enables a principled modification that benefits detection latency and mode consistency without losing computational tractability.

The rest of the paper is organized as follows: Sec. II introduces the necessary mathematical prerequisites. Sec. III presents the proposed approach based on IMM-KF. Sec. IV shows the simulation results, along with experimental implementation results on an actual robot leg. Finally, Sec. V concludes the paper and highlights potential future directions.

## II. PRELIMINARIES

This section provides an overview of GMO, KF and IMM-KF.

### A. Generalized Momentum-based Disturbance Observer

The equations of motion of a robot leg with  $n$  joints, under an external force are

$$M(q)\ddot{q} + C(q, \dot{q})\dot{q} + G(q) = \tau + J^\top F_{\text{ext}}, \quad (1)$$

where  $q \in \mathbb{R}^n$  is the joint angles,  $M(q) \in \mathbb{R}^{n \times n}$  is the generalized mass matrix,  $C(q, \dot{q}) \in \mathbb{R}^n$  is the term due to Coriolis and centrifugal forces,  $G(q) \in \mathbb{R}^n$  is the term due to gravity,  $\tau \in \mathbb{R}^n$  is the vector of joint torques,  $J \in \mathbb{R}^{3 \times n}$  and  $F_{\text{ext}}$  is the external force on the foot.

The Generalized Momentum (GM) is defined as

$$p = M(q)\dot{q}. \quad (2)$$

Using the skew-symmetry property of the robot, the dynamics of the GM can be calculated as

$$\dot{M}(q) = C(q, \dot{q}) + C^\top(q, \dot{q}). \quad (3)$$

The dynamics of the GM can be formed as

$$\dot{p} = C^\top(q, \dot{q})\dot{q} - G(q) + \tau + J^\top F_{\text{ext}}. \quad (4)$$

### B. Linear Kalman Filter

A linear Kalman filter is a recursive state estimator based on minimizing the Mean Square Error (MSE) for a dynamical system in the form

$$x_{k+1} = A_k x_k + B_k u_k + w_k \quad (5)$$

$$y_k = C_k x_k + v_k, \quad (6)$$

where  $x_k \in \mathbb{R}^n$  is the vector of system states at sample  $k$ ,  $u_k$  is the control input to the system,  $w_k \sim \mathcal{N}(0, Q_k)$  is the process noise, and  $v_k \sim \mathcal{N}(0, R_k)$  is the measurement noise.

The estimation is composed of two steps:

- Prediction:

In this step, the estimation of the states is updated using only the knowledge of the dynamics.

$$\hat{x}_k^- = A_{k-1} \hat{x}_{k-1}^+ + B_{k-1} u_{k-1}, \quad (7)$$

$$P_k^- = A_{k-1} P_{k-1}^+ A_{k-1}^\top + Q_{k-1}, \quad (8)$$

where  $\hat{x}_k^- \in \mathbb{R}^n$  denotes the a priori estimation of the states at sample  $k$ , and  $P_k^-$  denotes the a priori matrix of covariance of estimation.

- Update: After the sensor measures the output, an update step is executed.

$$\tilde{y}_k = y_k - C \hat{x}_k^-, \quad (9)$$

$$S_k = C_k P_k^- C_k^\top + R_k, \quad (10)$$

$$K_k = P_k^- C_k^\top S_k^{-1}, \quad (11)$$

$$\hat{x}_k^+ = \hat{x}_k^- + K_k \tilde{y}_k, \quad (12)$$

$$P_k^+ = (I - K_k C_k) P_k^-, \quad (13)$$

### C. Interacting Multiple-Model Kalman Filter

A robotic leg can have different modes: it can be in swing, in stance or in collision with the environment. This encourages the use of IMM-KF to estimate the mode simultaneously with the force.

Consider a system with  $M$  linear modes. For mode  $i$ , the dynamics are

$$x_k^{(i)} = A^{(i)} x_{k-1}^{(i)} + B^{(i)} u_{k-1} + w_k^{(i)}, \quad (14)$$

$$y_k^{(i)} = C^{(i)} x_k^{(i)} + v_k^{(i)}. \quad (15)$$

The mode  $m_k \in \{1, \dots, M\}$  evolves according to a Markov chain with transition probabilities

$$\pi_{ij} = \Pr(m_k = j \mid m_{k-1} = i). \quad (16)$$

Let  $\mu_{k-1}^{(i)}$  denote the mode probability at time  $k-1$ , and  $(\hat{x}_{k-1}^{(i)}, P_{k-1}^{(i)})$  the corresponding state estimate and covariance.

- Interaction Step:

In this step, for each mode  $j$ , the following is calculated:

$$\bar{\mu}_{k-1}^{(j)} = \sum_{i=1}^M \pi_{ij} \mu_{k-1}^{(i)}, \quad (17)$$

$$\mu_{k-1}^{(i|j)} = \frac{\pi_{ij} \mu_{k-1}^{(i)}}{\bar{\mu}_{k-1}^{(j)}}, \quad (18)$$

$$\bar{x}_{k-1}^{(j)} = \sum_{i=1}^M \mu_{k-1}^{(i|j)} \hat{x}_{k-1}^{+(i)}, \quad (19)$$

$$\bar{P}_{k-1}^{(j)} = \sum_{i=1}^M \mu_{k-1}^{(i|j)} \left[ P_{k-1}^{+(i)} + \hat{X}_{k-1}^{(i,j)} \right], \quad (20)$$

where  $\hat{X}_{k-1}^{(i,j)} = (\bar{x}_{k-1}^{(i)} - \hat{x}_{k-1}^{+(j)})(\bar{x}_{k-1}^{(i)} - \hat{x}_{k-1}^{+(j)})^\top$ .

- **Mode-Conditioned Filtering:**

For each mode  $j$ , a standard Kalman filter is initialized with  $\bar{x}_{k-1}^{(j)}$  and  $P_{k-1}^{+(j)}$ ; one prediction and one update step is performed and  $S_k^{(j)}$ ,  $\tilde{y}_k^{(j)}$ ,  $\hat{x}_k^{+(j)}$  and  $P_k^{+(j)}$  are calculated.

- **Mode Probability Update:**

The likelihood of mode  $j$  is

$$\Lambda_k^{(j)} = \mathcal{N}(\tilde{y}_k^{(j)}; 0, S_k^{(j)}). \quad (21)$$

The updated mode probability is

$$\mu_k^{(j)} = \frac{\Lambda_k^{(j)} \bar{\mu}_{k-1}^{(j)}}{\sum_{\ell=1}^M \Lambda_k^{(\ell)} \bar{\mu}_{k-1}^{(\ell)}}. \quad (22)$$

- **Combination:**

The overall state estimate and covariance are then obtained by

$$\hat{x}_k^+ = \sum_{j=1}^M \mu_k^{(j)} \hat{x}_k^{+(j)}, \quad (23)$$

$$P_k^+ = \sum_{j=1}^M \mu_k^{(j)} \left[ P_k^{+(j)} + \Gamma_k^{(j)} \right], \quad (24)$$

with  $\Gamma_k^{(j)} = (\hat{x}_k^{+(j)} - \hat{x}_k^+)(\hat{x}_k^{+(j)} - \hat{x}_k^+)^{\top}$ .

### III. FORCE ESTIMATION AND MODE DETECTION

One way to estimate the external force is to use the generalized momentum introduced in Sec. II. The generalized momentum can be constructed by (2) using the measurements of the joint angles and velocities. The only unknown in the right-hand side of (4) is the external force  $F_{\text{ext}}$ , which can then be estimated; however, due to the inherent noise in measuring the joint angles, and especially the joint velocities, the estimation of force is very noisy.

#### A. Filtered Force Estimation Methods

To handle the large noise in the estimated force, a handful of solutions have been proposed. In [9], a first-order continuous-time filter was used in the form

$$\hat{\tau}_c = \lambda p - \frac{\lambda}{s + \lambda} (\lambda p + \tau + C^\top \dot{q} - G), \quad (25)$$

where the subscript  $c$  denotes continuous-time domain. In [14], the authors proposed a discrete-time equivalent to (25), by calibrating the coefficients to be consistent with the inevitably discrete-time implementation of the algorithm:

$$\hat{\tau}_d = \beta p - \frac{1 - \gamma}{1 - \gamma z^{-1}} (\beta p + \tau + C^\top \dot{q} - G). \quad (26)$$

Another approach to getting a smoother estimation of the external force is to use a Kalman filter. In [15], the following linear system was formed:

$$\begin{bmatrix} \dot{p} \\ \dot{F}_{\text{ext}} \end{bmatrix} = \begin{bmatrix} 0 & J^\top \\ 0 & A_F \end{bmatrix} \begin{bmatrix} p \\ F_{\text{ext}} \end{bmatrix} + \begin{bmatrix} I \\ 0 \end{bmatrix} u + \begin{bmatrix} w_p \\ w_F \end{bmatrix}, \quad (27)$$

$$p = M \dot{q} + w_m. \quad (28)$$

where  $u = C^\top (q, \dot{q}) \dot{q} - G(q) + \tau$ , and a simple first-order dynamic is assumed for the force. Then a linear Kalman filter was used to estimate the external force. In each sample, the momentum is reconstructed using the measurements of joint angles and angular velocities.  $w_p$  accounts for the deviations from the rigid body assumptions and inaccuracies in the robot parameters, and  $w_F$  represents the uncertainty associated with the first-order dynamics assumed for the force.

The above methods all estimate a non-zero force when the foot is in the air, which is not ideal, because it can lead to false contact detection. Due to the limitations discussed in Sec. I, detecting contact and thus mode, by applying a threshold on the estimated external force is not ideal. To deal with this, in [18], an IMM was proposed to simultaneously estimate force and detect collisions, but the authors used a constant TPM. In this work, we propose a method to use the kinematics and force estimation information

#### B. Proposed Method

To address the limitations discussed above, we employ an IMM-based framework to simultaneously estimate the external force and detect the contact mode. The estimator considers three modes: swing, stance, and collision. Following the formulation used in previous momentum-based force estimators, a selection multiplier  $S$  is used in the system dynamics to account for the presence or absence of contact forces. The resulting model is written as

$$\begin{bmatrix} \dot{p} \\ \dot{F}_{\text{ext}} \end{bmatrix} = \begin{bmatrix} 0 & S J^\top \\ 0 & A_F \end{bmatrix} \begin{bmatrix} p \\ F_{\text{ext}} \end{bmatrix} + \begin{bmatrix} I \\ 0 \end{bmatrix} u + \begin{bmatrix} w_p \\ w_F \end{bmatrix} \quad (29)$$

where  $S = 0$  for the swing mode, and  $S = I$  for the stance and collision modes. For better distinction between different contact modes, a pseudo-force measurement is used in addition to the generalized momentum measurement. When the foot is in contact and assuming no slip, the contact constraint is

$$J \ddot{q} + \dot{J} \dot{q} = 0, \quad (30)$$

from which the pseudo-measurement can be constructed as

$$F_{\text{pf}} = - (J M^{-1} J^\top)^\dagger (J M^{-1} \tau + \dot{J} \dot{q}) + w_{\text{pf}}. \quad (31)$$

The covariance of this measurement,  $w_{pf}$ , is set to a large value if the estimated force lies within the current mode's friction cone, or a small value otherwise. Stance and collision modes are differentiated based on their friction cones: the stance friction cone is aligned with the vertical axis normal to the ground, whereas the collision friction cone is aligned with the horizontal axis.

Instead of relying on heuristics or manual tuning to find the appropriate TPM, we propose a new method to update the elements of TPM based on the current mode, swing phase and force estimation. In addition, a tuning parameter  $0 \leq \alpha \leq 1$  is proposed, which represents the uncertainty about the terrain. In an indoor or laboratory environment,  $\alpha$  can be set close to zero, and in outdoors environments,  $\alpha$  can be set closer to one.

The TPM is the matrix in which the transition probabilities  $\pi_{ij}$  are defined to be used in (16). The proposed TPM is defined as:

$$\Pi = \begin{bmatrix} \pi_{\text{swing}} & \frac{1-\pi_{\text{swing}}}{2} & \frac{1-\pi_{\text{swing}}}{2} \\ 1-\pi_{\text{stance}} & \pi_{\text{stance}} & 0 \\ 1-\pi_{\text{collision}} & 0 & \pi_{\text{collision}} \end{bmatrix}, \quad (32)$$

in which the following diagonal entries are used

$$\pi_{\text{swing}} = 0.45 \left( \operatorname{erf}\left(\frac{\phi_s - \mu_0}{\sigma\sqrt{2}}\right) + \operatorname{erf}\left(\frac{\mu_1 - \phi_s}{\sigma\sqrt{2}}\right) \right), \quad (33)$$

$$\pi_{\text{stance}} = 0.5 + \frac{0.45}{1 + e^{\frac{-f_x}{3(\alpha+1)} + 4}}, \quad (34)$$

$$\pi_{\text{collision}} = 0.5 + \frac{0.45}{1 + e^{\frac{-f_x}{3(\alpha+1)} + 4}}, \quad (35)$$

where  $\sigma = 0.13 + 0.5\alpha$  controls the spread of the swing-phase probability,  $\phi_s$  denotes the swing phase, and  $\mu_0$  and  $\mu_1$  denote the start (0) and end (1) of the swing phase, respectively. The function  $\operatorname{erf}(\cdot)$  is the Gauss error function, defined as

$$\operatorname{erf}(x) = \frac{2}{\sqrt{\pi}} \int_0^x e^{-t^2} dt. \quad (36)$$

For the swing mode, more probability is given to switching to another mode if it is near the beginning or the end of the swing. This basically means that in the middle of the swing phase, when the foot is higher in the air, there is less chance of colliding with an obstacle or going into stance mode. For the stance and collision modes, the estimated force appears in the TPM. The larger the estimated force, the less chance that the foot will transition to swing phase right in the next sample. Increasing  $\alpha$  reduces  $\pi_{\text{swing}}$  in the swing phase and decreases  $\pi_{\text{stance}}$  and  $\pi_{\text{collision}}$  for a given force. Consequently, larger values of  $\alpha$  make the estimator more responsive to mode transitions when terrain information is unreliable, while smaller  $\alpha$  values lead to more conservative switching and stronger reliance on terrain information.

#### IV. RESULTS

To show the efficacy of the proposed approach, we test the method in both simulation and on a self-developed single robot leg on a test stand. The robot has two degrees of freedom in the hip and the knee. The thigh and the shank

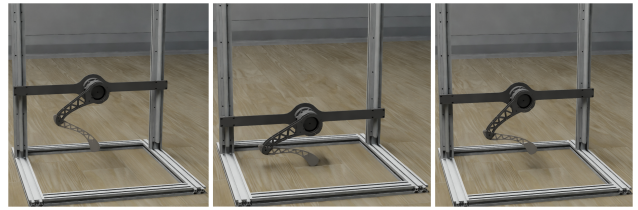


Fig. 2. Isaac Sim environment used for simulation experiments.

links are 21.3 cm and 23.0 cm and they weigh 0.8 kg and 0.2 kg, respectively.

It is worth noting that during collision, the external force has negligible effects on the trunk and other legs of a quadrupedal robot [18]; therefore a quadrupedal leg acts like a single leg as well.

#### A. Simulation Results

The resulting external force estimations are shown in Fig. 1.

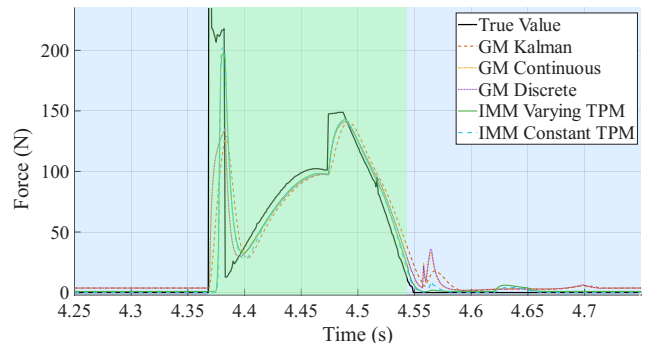


Fig. 1. Estimation of external force using different methods in Isaac Sim environment. Blue and green regions show swing and stance mode, respectively.

Simulations were conducted in the Isaac Sim environment, illustrated in Fig. 2. These simulations serve two purposes: to validate that our implementation closely estimates the true external force provided by the simulator, and to compare our proposed method with other approaches, which are introduced in the next subsection. As can be seen, the proposed method exhibits smaller fluctuations during the swing phase when estimating the external force.

#### B. Experimental Results

The proposed method was also tested on an actual robot leg. A pneumatic pressure sensor was used as ground truth

TABLE I  
PERFORMANCE COMPARISON OF MODELS

Method	Swing RMSE (N)	Delay (ms)
GM Continuous	1.99	13.87
GM Discrete	1.99	13.25
GM Kalman	2.07	27.00
IMM Constant TPM	0.27	23.12
Proposed	0.39	10.25

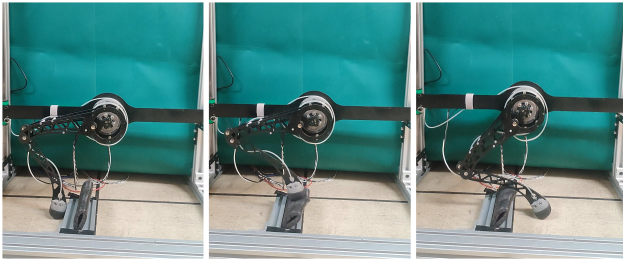


Fig. 3. Real Experiment Setup.

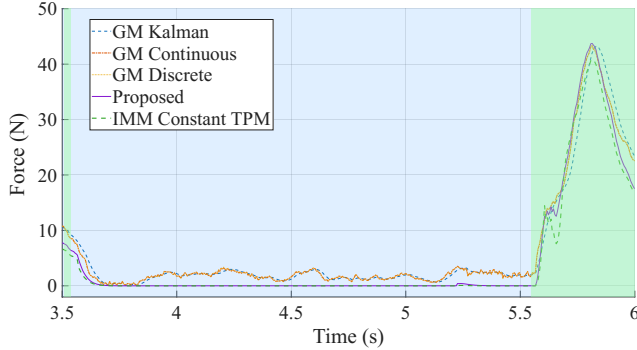


Fig. 4. Estimation of external force using different methods. Blue and green regions show swing and stance mode, respectively.

for validating the force estimations. All computations were done on a desktop PC with a Core i5-14400F CPU and an Nvidia GeForce RTX 3080 graphics card. The setup is shown in Fig. 3.

Two sets of experiments were conducted. In the first set, the leg started in stance mode, followed a swing trajectory generated by a Bézier curve, and returned to stance mode. The resulting estimated forces and mode probabilities are shown in Fig. 4 and Fig. 5, respectively. Shaded regions indicate swing and stance phases in blue and green, determined using a 10 N threshold on the force measured by the sensor. A summary of the results after 29 gait cycles is also presented in Table I. Fig. 6 additionally shows how the diagonal entries of the TPM change with different values of  $\alpha$ . The proposed method was compared with four other approaches:

- GM Continuous, from [9],
- GM Discrete, from [14],
- GM Kalman, from [15],
- IMM Constant TPM, from [18],

In the second set of experiments, a soft obstacle was placed in the middle of the swing phase to evaluate the effect of the parameter  $\alpha$  (see Fig. 3). The proposed method was tested with different  $\alpha$  values, and the resulting mode probabilities and estimated force are shown in Fig. 7 and Fig. 8, respectively.

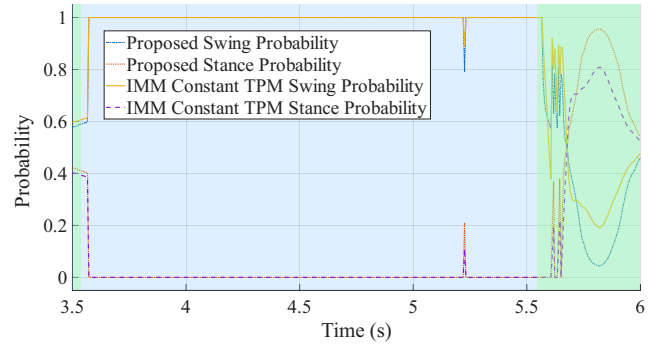


Fig. 5. Probability of different modes. Blue and green regions show swing and stance mode, respectively.

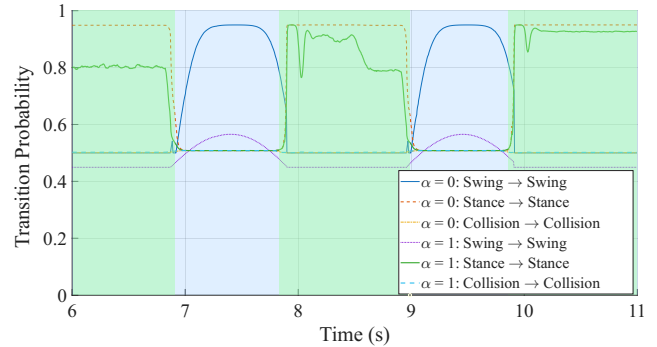


Fig. 6. Diagonal entries of the TPM for two values of  $\alpha$ . Blue and green regions show swing and stance mode, respectively.

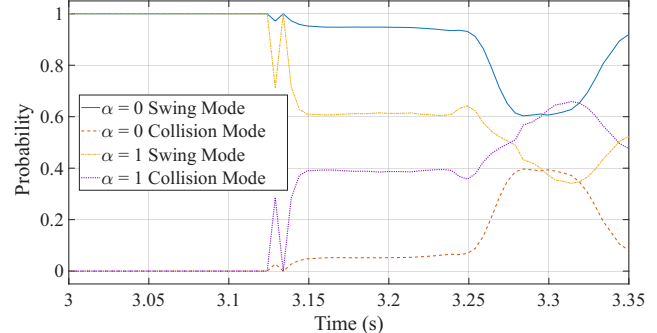


Fig. 7. Probability of different modes with different values of  $\alpha$ .

### C. Discussion

In the first set of experiments, Table I shows that methods not using the selection multiplier exhibit non-zero force estimates during the swing phase, which can lead to false contact detections. In contrast, the proposed method outperforms the approach with a constant TPM, as it leverages additional kinematic and dynamic information to improve contact detection and, consequently, force estimation accuracy.

The effect of the terrain uncertainty parameter  $\alpha$  was also investigated. Smaller values of  $\alpha$  (e.g.,  $\alpha \approx 0$ ) indicate high confidence in terrain information, resulting in smoother force estimates during swing and timely detection of stance phases, but potentially delayed collision detection. Larger values of  $\alpha$  (e.g.,  $\alpha \approx 1$ ) correspond to higher terrain uncertainty, which

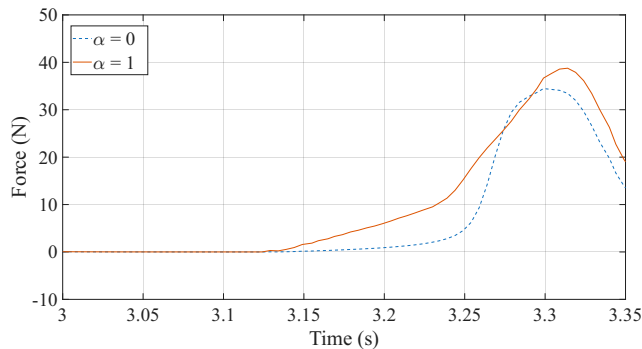


Fig. 8. Estimation of external force with variable  $\alpha$ .

accelerates collision detection but increases fluctuations in the estimated force.

The second set of experiments, designed to evaluate the influence of  $\alpha$ , highlights how this parameter affects collision detection. As shown in Fig. 7, with  $\alpha = 0$  the estimator treats the soft obstacle as non-colliding, whereas with  $\alpha = 1$  it registers a collision. This indicates that, depending on the environment in which the robot operates,  $\alpha$  can be set to ensure appropriate sensitivity: for instance, in outdoor areas with soft obstacles such as grass or mud, a lower  $\alpha$  can prevent unnecessary collision detection, while in more rigid environments, a higher  $\alpha$  ensures timely detection of significant impacts. Moreover, as illustrated in Fig. 8, increasing  $\alpha$  makes the estimator more sensitive and responsive in force estimation, allowing it to detect and estimate contact forces earlier compared with lower  $\alpha$  values. However, this increased sensitivity also leads to the identification of collisions in situations where softer contacts occur.

## V. CONCLUSION

This paper presented a probabilistic approach to the estimation of external forces and the determination of contact modes of a quadruped robot. To this end, an interacting multiple model Kalman filter with a time-varying transition probability matrix was used. Contrary to the conventional approach to the implementation of the IMM-KF, in which constant transition probabilities are used, the proposed approach utilizes the gait phase and the information obtained from the estimation of the forces. A terrain uncertainty parameter,  $\alpha$ , was also introduced, allowing the estimator to adjust its responsiveness according to the environment. In particular,  $\alpha$  can be adapted in outdoor or soft terrain conditions to prevent unwanted collision or stance detections. The proposed method was tested on a real robot and a comparison with the conventional approaches to the estimation of external forces and the determination of the contact modes has been carried out. It has been shown that the proposed approach yields better results in the estimation of the external forces while maintaining the quality of the transitions between the contact modes. Future work will explore the integration of exteroceptive sensing, such as vision or terrain classification, directly into the transition modeling process. In addition, adaptive strategies for online tuning of the terrain uncertainty

parameter will be investigated to further enhance robustness in highly dynamic environments.

## REFERENCES

- [1] F. Jenelten, T. Miki, A. E. Vijayan, M. Bjelonic, and M. Hutter, "Perceptive locomotion in rough terrain—online foothold optimization," *IEEE Robotics and Automation Letters*, vol. 5, no. 4, pp. 5370–5376, 2020.
- [2] M. Bloesch, M. Hutter, M. Hoepflinger, S. Leutenegger, C. Gehring, C. D. Remy, and R. Siegwart, "State estimation for legged robots – consistent fusion of leg kinematics and IMU," in *Proceedings of Robotics: Science and Systems*, Sydney, Australia, Jul. 2012.
- [3] M. Camurri, M. Ramezani, S. Nobili, and M. Fallon, "Pronto: A multi-sensor state estimator for legged robots in real-world scenarios," *Frontiers in Robotics and AI*, vol. 7, p. 68, 2020.
- [4] J. Hwangbo, C. D. Bellicoso, P. Fankhauser, and M. Hutter, "Probabilistic foot contact estimation by fusing information from dynamics and differential/forward kinematics," in *2016 IEEE/RSJ International Conference on Intelligent Robots and Systems (IROS)*. IEEE, 2016, pp. 3872–3878.
- [5] M. Maravagakis, D. Argiropoulos, S. Piperakis, and P. Trahanias, "Probabilistic contact state estimation for legged robots using inertial information," in *Proceedings of IEEE International Conference on Robotics and Automation (ICRA)*, 2023.
- [6] J. Kang and X. Xiong, "Simultaneous ground reaction force and state estimation via constrained moving horizon estimation," in *2025 IEEE International Conference on Robotics and Automation (ICRA)*. IEEE, 2025, pp. 7080–7086.
- [7] Z. Cong, A. Honglei, C. Wu, L. Lang, Q. Wei, and M. Hongxu, "Contact force estimation method of legged-robot and its application in impedance control," *IEEE Access*, vol. 8, pp. 161 175–161 187, 2020.
- [8] F. Lin, T. Zhang, X. Xiong, and Y. Lou, "Transformer observer-based contact force estimation for quadruped manipulators with model uncertainties," *IEEE Robotics and Automation Letters*, vol. 11, no. 2, pp. 1914–1921, 2026.
- [9] A. De Luca, A. Albu-Schaffer, S. Haddadin, and G. Hirzinger, "Collision detection and safe reaction with the dlr-iii lightweight manipulator arm," in *2006 IEEE/RSJ international conference on intelligent robots and systems*. IEEE, 2006, pp. 1623–1630.
- [10] G. Fink and C. Semini, "Proprioceptive sensor fusion for quadruped robot state estimation," in *2020 IEEE/RSJ International Conference on Intelligent Robots and Systems (IROS)*, 2020, pp. 10914–10920.
- [11] D. Youm, H. Oh, S. Choi, H. Kim, S. Jeon, and J. Hwangbo, "Legged robot state estimation with invariant extended kalman filter using neural measurement network," in *2025 IEEE International Conference on Robotics and Automation (ICRA)*, 2025, pp. 670–676.
- [12] Y. Nisticò, J. C. V. Soares, L. Amatucci, G. Fink, and C. Semini, "Muse: A real-time multi-sensor state estimator for quadruped robots," *IEEE Robotics and Automation Letters*, vol. 10, no. 5, pp. 4620–4627, 2025.
- [13] M. Camurri, M. Fallon, S. Bazeille, A. Radulescu, V. Barasuol, D. G. Caldwell, and C. Semini, "Probabilistic contact estimation and impact detection for state estimation of quadruped robots," *IEEE Robotics and Automation Letters*, vol. 2, no. 2, pp. 1023–1030, Apr. 2017.
- [14] G. Bledt, P. M. Wensing, S. Ingersoll, and S. Kim, "Contact model fusion for event-based locomotion in unstructured terrains," in *2018 IEEE International Conference on Robotics and Automation (ICRA)*. IEEE, 2018, pp. 4399–4406.
- [15] W. Deng, Y. Xu, Q. Yuan, X. Lv, G. Xie, and P. Li, "Foot-end contact state estimation for quadruped robots based on proprioceptive sensing," *Measurement Science and Technology*, vol. 36, no. 6, p. 066209, 2025.
- [16] S. Teng, M. W. Mueller, and K. Sreenath, "Legged robot state estimation in slippery environments using invariant extended kalman filter with velocity update," in *Proceedings of the IEEE International Conference on Robotics and Automation (ICRA)*, 2021, pp. 3104–3110.
- [17] M. Menner and K. Berntorp, "Simultaneous state estimation and contact detection for legged robots by multiple-model kalman filtering," in *2024 European Control Conference (ECC)*, 2024, pp. 2768–2773.
- [18] Z. Zhou, S. Di Cairano, Y. Wang, and K. Berntorp, "Simultaneous collision detection and force estimation for dynamic quadrupedal locomotion," in *2025 IEEE International Conference on Robotics and Automation (ICRA)*. IEEE, 2025, pp. 691–697.